

Competing dynamics in the one-dimensional Blume-Emery-Griffiths model: Hydrodynamic equations

J. F. F. Mendes* and E. J. S. Lage *

Departamento de Física da Universidade do Porto, Praça Gomes Teixeira, 4000 Porto, Portugal

(Received 13 January 1993)

We study the one-dimensional Blume-Emery-Griffiths model, subjected to a combination of Glauber (reaction) and Kawasaki (diffusion) dynamics. The Glauber rate satisfies detailed balance at a temperature β^{-1} , while the Kawasaki rate randomly exchanges nearest-neighbor spins. We obtain the *hydrodynamic equations* for the two order parameters m (magnetization) and q (quadrupolar ordering). We also present the phase diagram and other macroscopic properties, namely, continuous and discontinuous phase transitions in the limit of infinitely fast exchanges.

PACS number(s): 64.60.-i, 05.50.+q, 05.70.Ce, 75.10.Hk

I. THE MODEL: DEFINITIONS

There has been much progress in recent years in deriving macroscopic equations [1] for systems whose microscopic dynamics involve some stochastic elements, e.g., particles (spins) on a lattice with stochastic dynamics. These systems usually have some conserved quantities, for which the stochastic dynamics maintains a local equilibrium distribution. One way to formulate a stochastic microscopic dynamics that generates these macroscopic equations is through competing dynamics [2], where the properties of the stationary states are no longer equilibrium Gibbs states. Some questions can arise about these nonequilibrium systems that exhibit phase transitions: *How do parameters such as the rate ratio, ϵ , of the microscopic time scales of competing dynamics, the range of the exchanges, etc., affect the various types of phase transitions?* A few results are known in this context. In the two-dimensional (2D) Ising case it was shown by González-Miranda and Marro [3] that for $\epsilon > \epsilon^*$ the system presents a continuous phase transition, otherwise for $\epsilon < \epsilon^*$ they observe a discontinuous one. Other nonequilibrium systems are known to exhibit discontinuous phase transitions, as in the case of the *autocatalytic chemical models* [4] where a discontinuous transition is observed for $d = 4$ (upper critical dimension). Another model is the stochastic cellular automata devised by Bidaux, Boccara, and Chaté [5], occurring for $d \geq 2$, but continuous for $d = 1$. The only known 1D model presenting first-order phase transition is the one proposed by Dickman and Tomé [6], competing diffusion and multiparticle annihilation. Here we present a 1D model which exhibits a rich phase diagram with first and second phase transitions, even in the limit $\epsilon \rightarrow 0$. This model consists of a system with three states per spin ($\sigma = \pm 1, 0$), known as the Blume-Emery-Griffiths (BEG) model [7] with reduced Hamiltonian $\mathcal{H}(\sigma)$ given by

$$-\beta\mathcal{H}(\sigma) = \sum_{x=1}^N [J\sigma_x\sigma_{x+1} + K\sigma_x^2\sigma_{x+1}^2 - D\sigma_x^2]. \quad (1.1)$$

The spin configuration $\sigma = \{\sigma_x : x \in \mathbb{Z}^1, \sigma = \pm 1, 0\}$

evolves in time due to a combination of a spin-flip (Glauber [8]) process in contact with a heat bath at temperature β^{-1} and a diffusion process (Kawasaki [9]) defined for nearest-neighbor (NN) exchanges, with a different associated bath temperature β'^{-1} . This rate will be assumed to be much faster than the spin flip. This model was also studied by us using Monte Carlo simulations for arbitrary finite rates and range of the exchanges [10]. The two-state, per spin, version of this model was studied by De Masi, Ferrari, and Lebowitz [11] in the limit $\epsilon \rightarrow 0$, by Dickman [13] using a mean-field approximation for arbitrary ϵ , and by Droz, Rácz, and Tartaglia [14] using Monte Carlo simulations.

Under these assumptions, the configurational probability distribution for the system, $P_\epsilon^{\beta\beta'}(\sigma; t)$, evolves in time according to the following master equation:

$$\frac{dP_\epsilon^{\beta\beta'}(\sigma; t)}{dt} = (L_G^\beta + \epsilon^{-2}L_K^{\beta'})P_\epsilon^{\beta\beta'}(\sigma; t) \quad (1.2)$$

where

$$L_G^\beta = \sum_x \sum_{\sigma_x} (\hat{p}_G^x - 1)c^\beta(x, \sigma), \quad (1.3)$$

$$L_K^{\beta'} = \sum_{|x-y|=1} (\hat{p}_K^{xy} - 1)c^{\beta'}(x, y, \sigma). \quad (1.4)$$

The operators \hat{p}_G^x and \hat{p}_K^{xy} act on an arbitrary function of the configuration by respectively flipping the spin at site x , or exchanging the two spins, at points x and y . As mentioned before, L_G^β is the generator for a Glauber-type dynamics and $L_K^{\beta'}$ is the generator for the exchange process. The rates associated with these processes $c^\beta(x; \sigma)$ and $c^{\beta'}(x, y; \sigma)$ both satisfy detailed balance at two different inverse temperatures β and β' . As a consequence,

$$L_G^\beta P_{\text{eq}}^\beta(\sigma) = 0, \quad (1.5)$$

with

$$P_{\text{eq}}^\beta(\sigma) = \left[\sum_{\sigma} \exp[-\beta\mathcal{H}(\sigma)] \right]^{-1} \exp[-\beta\mathcal{H}(\sigma)],$$

and

$$L_K^{\beta'} P_{\text{eq}}^{\beta'}(\boldsymbol{\sigma}; m, q) = 0, \quad (1.6)$$

where $P_{\text{eq}}^{\beta'}(\boldsymbol{\sigma}; m, q)$ is the Gibbs state at inverse temperature β' , corresponding to fixed values for the magnetization m and quadrupolar average q . Finally, the parameter ϵ in Eq. (1.2) just measures the ratio of the intrinsic microscopic time scales associated with the two different dynamic processes.

II. HYDRODYNAMIC REGIME ($\epsilon \rightarrow 0$)

A. General results

There are several limits where it is possible to derive macroscopic equations from underlying microscopic evolutions, under appropriate space-time (hydrodynamic) scaling [15]. These equations arise for very fast exchanges ($\epsilon \rightarrow 0$), leading to a scaling of times by ϵ^{-2} and of length by ϵ^{-1} . In this limit the macroscopic local quantities satisfy a couple of *reaction-diffusion* equations.

Hereafter, we shall only consider the case of $\beta' = 0$ (completely random exchanges). In this case, the distribution $P_{\text{eq}}^{\beta'}(\boldsymbol{\sigma}; m, q)$ is a local equilibrium distribution, with spins distributed independently inside domains of length ϵ^{-1} in original NN distance.

Multiply Eq. (1.2) by σ_x or σ_x^2 and sum over the spins to obtain the respective dynamic evolution equations,

$$\begin{aligned} \frac{d}{dt} \langle \sigma_x^\alpha \rangle = & - \left\langle \sum_{\sigma'_x} (\sigma_x^\alpha - \sigma'_x{}^\alpha) c^\beta(x; \boldsymbol{\sigma}) \right\rangle \\ & + \epsilon^{-2} \sum_{z=x\pm 1} \langle (\sigma_z^\alpha - \sigma_x^\alpha) c^{\beta'}(x, z; \boldsymbol{\sigma}) \rangle, \end{aligned} \quad (2.1)$$

where $\alpha = 1, 2$. The averages here were taken with the distribution $P_\epsilon^{\beta'}(\boldsymbol{\sigma}; t)$. Let us define the magnetization and quadrupolar average densities on the scale ϵ^{-1} by

$$m_\epsilon(r; \boldsymbol{\sigma}) = \epsilon^{-1} \sum_{x \in \Omega_{r, \epsilon}} \sigma_x, \quad (2.2)$$

$$q_\epsilon(r; \boldsymbol{\sigma}) = \epsilon^{-1} \sum_{x \in \Omega_{r, \epsilon}} \sigma_x^2, \quad (2.3)$$

where $\Omega_{r, \epsilon}$ are domains of size ϵ^{-1} and centered at the point defined by r . Obviously two NN domains located at r and r' are separated by $a = \epsilon^{-1}$, which is our unit of length. The change in the quantities $m_\epsilon(r; \boldsymbol{\sigma})$ and $q_\epsilon(r; \boldsymbol{\sigma})$ in a fixed macroscopic interval of time arises from the number of flips inside $\Omega_{r, \epsilon}$, which is proportional to ϵ^{-1} , and from the exchanges through the boundaries of $\Omega_{r, \epsilon}$, that are proportional to the gradient ($\propto \epsilon$) of the $m_\epsilon(r; \boldsymbol{\sigma})$ or $q_\epsilon(r; \boldsymbol{\sigma})$, times ϵ^{-2} .

Using Eq. (2.2) and Eq. (2.3) we obtain

$$\begin{aligned} \frac{\partial m_\epsilon(r; t)}{\partial t} = & - \epsilon \left\langle \sum_{x \in \Omega_{r, \epsilon}} \sum_{\sigma'_x} (\sigma_x - \sigma'_x) c^\beta(x; \boldsymbol{\sigma}) \right\rangle + \epsilon^{-1} \left\langle \sum_{x \in \Omega_{r, \epsilon}} \sum_{z=x\pm 1} (\sigma_z - \sigma'_x) c^{\beta'}(x, z; \boldsymbol{\sigma}) \right\rangle, \\ \frac{\partial q_\epsilon(r; t)}{\partial t} = & - \epsilon \left\langle \sum_{x \in \Omega_{r, \epsilon}} \sum_{\sigma'_x} (\sigma_x^2 - \sigma'_x{}^2) c^\beta(x; \boldsymbol{\sigma}) \right\rangle + \epsilon^{-1} \left\langle \sum_{x \in \Omega_{r, \epsilon}} \sum_{z=x\pm 1} (\sigma_z^2 - \sigma'_x{}^2) c^{\beta'}(x, z; \boldsymbol{\sigma}) \right\rangle, \end{aligned} \quad (2.4)$$

$$m_\epsilon(r; t) \equiv \langle m_\epsilon(r; \boldsymbol{\sigma}) \rangle, \quad q_\epsilon(r; t) \equiv \langle q_\epsilon(r; \boldsymbol{\sigma}) \rangle.$$

In the limit $\epsilon \rightarrow 0$ there is a clear separation between the macroscopic and microscopic scales, and we expect that the exchanges that become infinitely fast on the macroscopic time scale compel the spins inside a domain to become independent, since an infinite number of exchanges takes place inside each domain, $\Omega_{r, \epsilon}$, during the time interval for a single spin flip. Simultaneously, as a consequence of $\epsilon \rightarrow 0$ the spin exchanges through the domain walls now have a negligible effect on the macroscopic quantities.

With these assumptions, the averages in Eqs. (2.4) may be taken with the distribution $P_0^{\beta'}(\boldsymbol{\sigma}; t) = \prod_r P_{\text{eq}}^{\beta'}(\boldsymbol{\sigma}_r; m(r; t), q(r; t))$, where $\boldsymbol{\sigma}_r$ corresponds to the spin configuration for the domain r . Then, the macroscopic time evolution for the order parameters takes the form

$$\frac{\partial m(r; t)}{\partial t} = - \left\langle \sum_{\sigma'_x} (\sigma_x - \sigma'_x) c^\beta(x; \boldsymbol{\sigma}) \right\rangle_{m, q} + \epsilon^{-2} \sum_{r'=r+a} \langle (\sigma_z - \sigma'_x) c^{\beta'}(x, z; \boldsymbol{\sigma}) \rangle_\pi, \quad (2.5)$$

$$\frac{\partial q(r; t)}{\partial t} = - \left\langle \sum_{\sigma'_x} (\sigma_x^2 - \sigma'_x{}^2) c^\beta(x; \boldsymbol{\sigma}) \right\rangle_{m, q} + \epsilon^{-2} \sum_{r'=r+a} \langle (\sigma_z^2 - \sigma'_x{}^2) c^{\beta'}(x, z; \boldsymbol{\sigma}) \rangle_\pi, \quad (2.6)$$

where $x \in \Omega_{r, \epsilon}$ and $z \in \Omega_{r', \epsilon}$, the average $\langle \rangle_{m, q}$ is taken with the distribution $P_{\text{eq}}^{\beta'}(\boldsymbol{\sigma}; m, q)$, and $\langle \rangle_\pi$ means an average taken with the product distribution $P_0^{\beta'}(\boldsymbol{\sigma}; t)$. If we

take the limit $\epsilon \rightarrow 0$ these evolution equations reduce to a couple of macroscopic reaction-diffusion equations, similar to those obtained by De Masi, Ferrari, and Lebowitz [11] for the Ising model.

B. Application

Here, we will derive explicitly the macroscopic evolution equations for given rates $c^\beta(x; \sigma)$ and $c^{\beta'}(x, y; \sigma)$ with $\beta' = 0$. The Glauber-type rate $c^\beta(x; \sigma)$ for inverse temperature β may be written in the following form:

$$c^\beta(x; \sigma) = \frac{1}{2} \left\{ 1 - \tanh \left[\frac{JS_1}{2} (\sigma_x - \sigma'_x) + \frac{KS_2 - D}{2} (\sigma_x^2 - \sigma'^2_x) \right] \right\}, \quad (2.7)$$

where $S_\alpha = \sigma_{x-1}^\alpha + \sigma_{x+1}^\alpha$. For the exchange process we consider $c^0(x, y; \sigma) = 1$. Using these rates and considering the homogeneous case (the diffusion term disappears) in Eq. (2.5) and Eq. (2.6) we obtain (see Appendix A)

$$\frac{dm}{dt} = A_1 m + B_1 m q + D_1 m q^2 + C_1 m^3, \quad (2.8)$$

$$\frac{dq}{dt} = A_2 + B_2 q + C_2 m^2 + D_2 q^2 + E_2 m^2 q + F_2 q^3 \quad (2.9)$$

(the coefficients are functions of J , K , and D , and are given in Appendix A), where m and q are site independent order parameters.

C. Stationary states: phase diagram

In this subsection, we will present a discussion of the previous polynomial equations in the stationary state. Equating the right-hand side of Eqs. (2.8) and (2.9) to zero, we may cast the equations in the following form:

$$\begin{aligned} 0 &= A_1 m + B_1 m q + D_1 m q^2 + C_1 m^3 = m f(m, q), \\ 0 &= A_2 + B_2 q + C_2 m^2 + D_2 q^2 + E_2 m^2 q + F_2 q^3 \\ &= (C_2 + E_2 q) m^2 + g(q). \end{aligned} \quad (2.10)$$

In what follows we shall consider three different phases, as they are usually defined for the BEG model in equilibrium [12].

- *Paramagnetic phase (P)*: $m = 0$, $q = 2/3$, equal number of spins in the three states.

- *Quadrupolar phase (Q)*: $m = 0$, $q \neq 2/3$, equal number of polarized spins ($\sigma = \pm 1$) and different number of zeros. The particular case $m = q = 0$ will characterize the totally quadrupolar phase (tQ).

- *Ferromagnetic phase (F)*: different number of spins in the two polarized states.

Also the order parameters have to obey the obvious condition,

$$|m| \leq q \leq 1. \quad (2.11)$$

The solutions were numerically investigated by using the computer and some appropriate numerical routines for this study. For each of the tested points in the phase space ($K/J, D/J$), we sweep the temperature (steps $\sim 10^{-5}$) to get the respective solution. They are studied in the following way.

- $m = 0$. This solution is always present. The cubic

equation for $g(q)$ has been found always to have only one real physical solution. This solution (henceforth, denoted by q_0) is obviously dependent on the temperature and the other Hamiltonian parameters. However, for $D = K = 0$, the analytical solution is found to be $q = 2/3$, independent of temperature. For other values of the parameters, the thermal behavior of q_0 falls into the two broad classes, typified by Fig. 2. Starting at infinite temperature ($q_0 = 2/3$) and decreasing the temperature, we find that either q_0 increases to $q = 1.0$ ($K/J < 0$) or decreases to $q = 0.0$ ($K/J > 0$). This suggests that well defined phases will be found at $T = 0$.

- $m \neq 0$. Some insight into the numerically found solutions may be obtained by performing an analysis similar to Landau's approach to equilibrium phase transitions. If we assume that m is small, we may then eliminate q between Eqs. (2.10) and obtain for the magnetization the equation,

$$0 = am + bm^3 + cm^5 + \dots \quad (2.12)$$

Here, the parameter-dependent coefficients a , b , and c are given in Appendix B.

We first consider the critical temperature defined by $a = 0$, that is, $A_1 + B_1 q_0 + D_1 q_0^2 = 0$. If b remains positive while T is decreased then the transition is continuous or second-order (dotted lines in the figures), since obviously only $m = 0$ at higher temperatures. Upon decreasing the temperature, this ferromagnetic phase may persist down to $T = 0$ or another critical line is found where one of the conditions in Eq. (2.11) is violated and therefore the system reenters the quadrupolar phase through a discontinuous or first-order phase transition (dashed line in the figures). Figures 2(a) and 2(b) illustrate the thermal dependence of the order parameters.

On the other hand, if b remains negative (near the point where a vanishes), then when T increases the system goes through a second-order phase transition. This ferromagnetic phase now persists until a new violation of

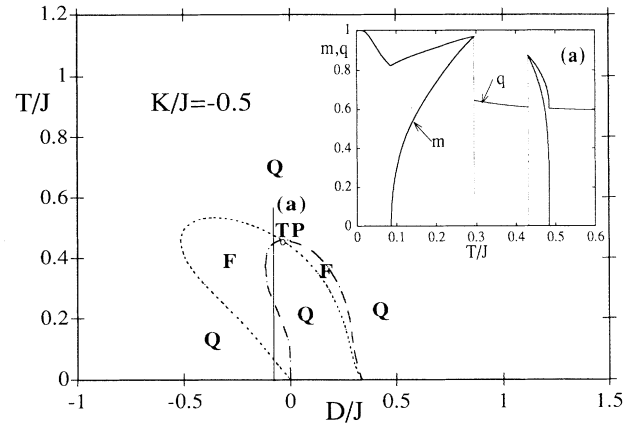


FIG. 1. Plot of the cross section T/J against D/J for $K/J = -0.5$. The inset shows the order parameters' variation with T/J along line (a). Dashed and dotted lines correspond respectively to discontinuous and continuous phase transitions.

Eq. (2.11) is found, whereby a strong first-order transition is observed and the system reenters the quadrupolar phase at higher temperatures [as shown, again, in Figs. 2(a) and 2(b)].

When these two transition lines meet, we identify this point as a tricritical point (TP in the figures). Alternatively, this point corresponds to $a = b = 0$. We now consider how these critical lines are affected by a change of the Hamiltonian parameters.

In Figs. 1, 2, and 3 we plot some sections of the phase diagram for different values of K/J . Figures 4 and 5 also show sections corresponding to constant values of D/J .

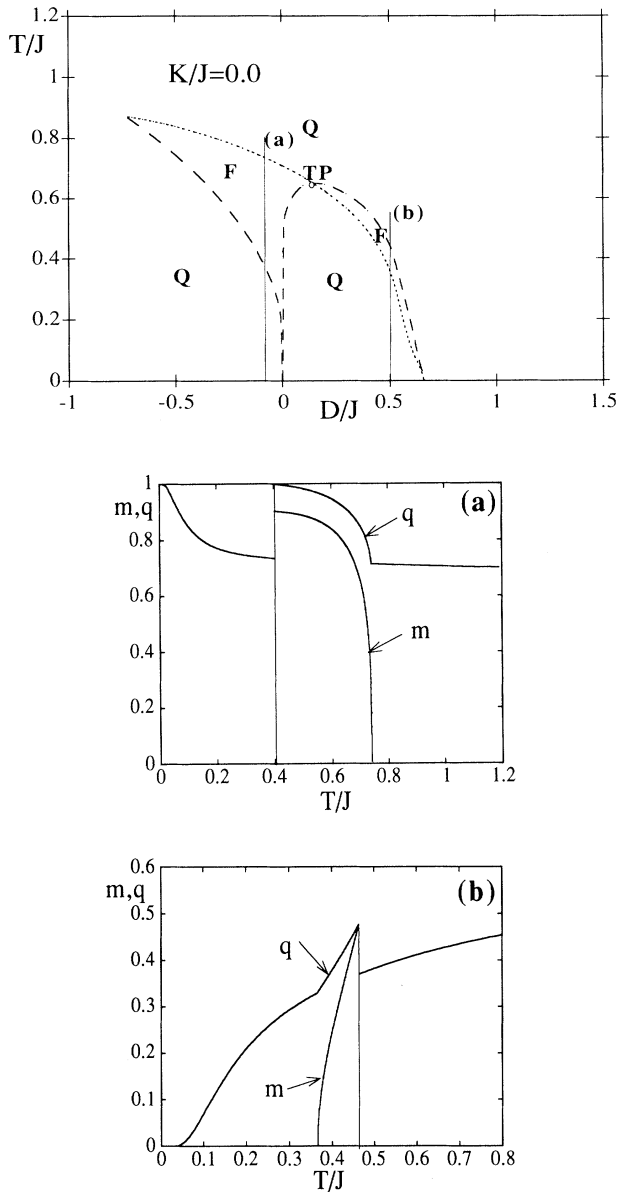


FIG. 2. Plot of the cross section T/J against D/J for $K/J = 0.0$. (a) The inset plot corresponds to the order parameters' variation with T/J in line (a). (b) The inset plot corresponds to the order parameters' variation with T/J in line (b).

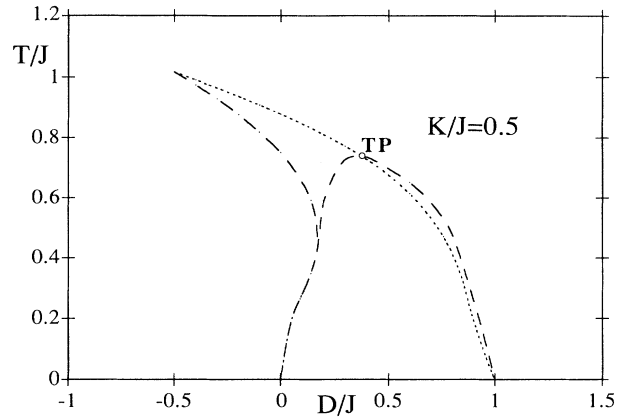


FIG. 3. Plot of the cross section T/J against D/J for $K/J = 0.5$.

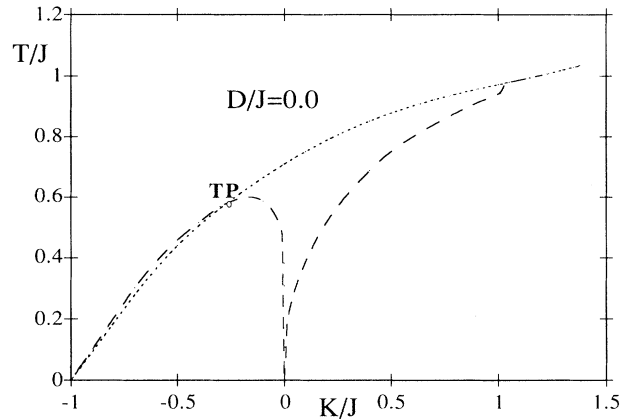


FIG. 4. Plot of the cross section T/J against K/J for $D/J = 0.0$.

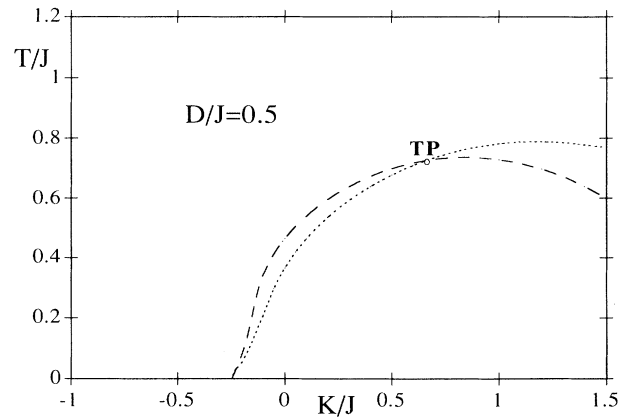


FIG. 5. Plot of the cross section T/J against K/J for $D/J = 0.5$.

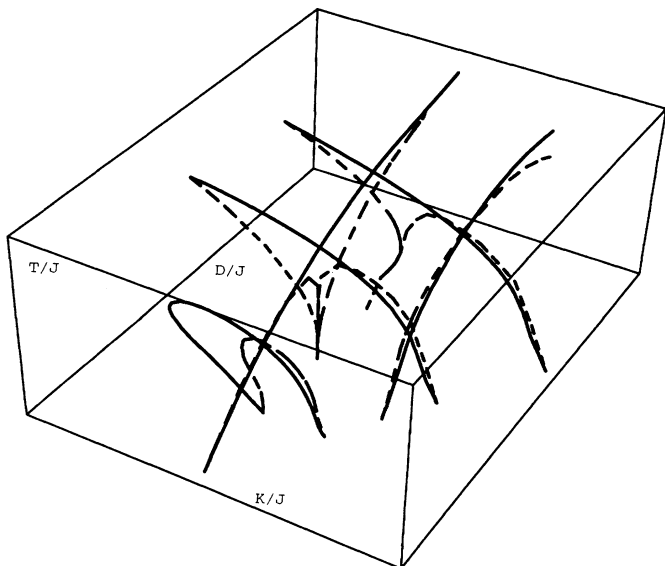


FIG. 6. Tridimensional representation of the phase diagram for several values of K/J and D/J .

Some different phases can be seen in these plots. For instance in Fig. 2 we see two distinct curves that intersect at a tricritical point. These critical lines correspond to the $(Q) \leftrightarrow (F) \leftrightarrow (Q)$ transition, when one decreases the temperature.

Consider Fig. 3. For $-0.5 < D/J < 0.0$ a ferromagnetic region appears, and at $T = 0$, $q = 1.0$. It is interesting to note that when the temperature is increased a first-order phase transition, $(Q) \leftrightarrow (F)$, is observed followed by a $(F) \leftrightarrow (Q)$ second-order type. The reverse happens in the region, $0 < D/J < 1.0$ and at $T = 0$ we have $q = 0.0$ (tQ). In Fig. 4, and at $T = 0$, we found that for $-1.0 < K/J < 0.0$, $q = 0.61804\dots$ and in the interval $0 < K/J < 1.38$, $q = 0.715225\dots$. For $K/J > 1.38$ there is no transition and q goes from $0.7966\dots$ at $T = 0$ to $2/3$ at $T = \infty$. Thus, for $D/J = 0.0$, the ground state does not correspond to a completely ordered phase. In Fig. 1, and for $-0.1164 < D/J < -0.036$, when

one increases the temperature from $T = 0$, four phase transitions were observed (see inset of Fig. 1); and the same happens for $-0.036 < D/J < 0.0$. The point $D/J = -0.036$ is a tricritical point.

Of course, since there is no free-energy functional to decide upon the relative stability of simultaneous phases, we cannot establish when exactly some of these phase transitions take place. For this reason, the sketched phase transition surfaces in Fig. 6, obtained from the numerically studied cross sections, must be considered as a tentative summary of the phase diagram.

III. CONCLUSION

We studied the one-dimensional BEG model subjected to a combination of two microscopic dynamics in the limit of completely random and faster exchanges, that is, the limit $\epsilon \rightarrow 0$ and infinite temperature for the exchanges.

We derived the reaction-diffusion equations for this model—they generalize the results found [11] for the Ising model, where only second-order phase transitions are observed. This Ising-like behavior is recovered for $D \rightarrow -\infty$ and $K = 0$. Some sections of the phase diagram were obtained, showing continuous and discontinuous transitions. We are then in the presence of a 1D model with a *starting Hamiltonian* that exhibits discontinuous transitions even in the limit $\epsilon \rightarrow 0$.

Two important points not discussed here are: how is the phase diagram affected when exchanges take place at finite temperature or when a different definition of the random microscopic exchanges is assumed. These will be matters for future work.

ACKNOWLEDGMENTS

J.F.F.M. acknowledges Professor P. A. Ferrari and Professor M. J. Oliveira for some helpful discussions. This work was supported in part by JNICT, Junta Nacional de Investigação Científica e Tecnológica, Project No. CEN-386/90. J.F.F.M. was supported in part by a grant from Instituto Nacional de Investigação Científica (INIC).

APPENDIX A

Here we present a more detailed derivation of Eqs. (2.8) and (2.9). Equation (2.7) may be cast in the following form:

$$c^\beta(x; \sigma) = \frac{1}{2} \left\{ 1 - \frac{1}{2} (\sigma_x - \sigma'_x) [(1 + \sigma_x)(1 + \sigma'_x) \tanh(A + B) + (1 - \sigma_x)(1 - \sigma'_x) \tanh(A - B) - \sigma_x \sigma'_x \tanh(2A)] \right\}, \quad (\text{A1})$$

with $A = JS_1/2$ and $B = (KS_2 - D)/2$.

Using the definition of S_1 and S_2 we have

$$\begin{aligned} \tanh(2A) &= \frac{1}{2} \sigma_{x-1} \sigma_{x+1} (\sigma_{x-1} + \sigma_{x+1}) \tanh(2J) + (\sigma_{x-1} + \sigma_{x+1}) (1 - \sigma_{x-1} \sigma_{x+1}) \tanh(J) \\ &= b_1 \tanh(2J) + b_2 \tanh(J) \end{aligned} \quad (\text{A2})$$

and also

$$\begin{aligned} \tanh(A + B) &= \tanh \left\{ \frac{J}{2} (\sigma_{x-1} + \sigma_{x+1}) + \frac{K}{2} (\sigma_{x-1}^2 + \sigma_{x+1}^2) - \frac{D}{2} \right\} \\ &= a_1 (\sigma_{x-1} + \sigma_{x+1}) + a_2 (\sigma_{x-1}^2 + \sigma_{x+1}^2) + a_3 \sigma_{x-1} \sigma_{x+1} + a_4 (\sigma_{x-1} \sigma_{x+1}^2 + \sigma_{x-1}^2 \sigma_{x+1}) + a_5 \sigma_{x-1}^2 \sigma_{x+1}^2 - a_6. \end{aligned} \quad (\text{A3})$$

Finally, $\tanh(A - B)$ may be formally obtained from $\tanh(A + B)$ by exchanging the sign of K and D . We obtain

$$\tanh(A - B) = a_1^*(\sigma_{x-1} + \sigma_{x+1}) + a_2^*(\sigma_{x-1}^2 + \sigma_{x+1}^2) + a_3^*\sigma_{x-1}\sigma_{x+1} + a_4^*(\sigma_{x-1}\sigma_{x+1}^2 + \sigma_{x-1}^2\sigma_{x+1}) + a_5^*\sigma_{x-1}^2\sigma_{x+1}^2 - a_6^*, \quad (\text{A4})$$

where $a_i^*(J, K, D) = a_i(J, -K, -D)$, $\forall i \in \{1, \dots, 6\}$. The coefficients a_i and a_i^* can be found easily by equating the left- and right-hand sides of Eq. (A3).

With these equations we obtain, for the time evolution of the order parameters, Eqs. (2.9) and (2.10), the respective coefficients given by

$$\begin{aligned} A_1 &= 2(a_1 + a_1^*) - \frac{1}{2}(a_6 - a_6^*) - 3, \\ B_1 &= 2(a_4 + a_4^*) - (a_1 + a_1^*) + (a_2 - a_2^*) + 4b_2, \\ C_1 &= \frac{1}{2}(a_3 + a_3^*), \\ D_1 &= \frac{1}{2}(a_5 - a_5^*) - (a_4 + a_4^*) + 4b_1, \\ A_2 &= 2 - (a_6 - a_6^*), \\ B_2 &= 2(a_2 - a_2^*) - \frac{1}{2}(a_6 - a_6^*) - 3, \\ C_2 &= (a_3 - a_3^*) + (a_1 + a_1^*), \\ D_2 &= (a_5 - a_5^*) - (a_2 + a_2^*), \\ E_2 &= (a_4 + a_4^*) - (a_3 - a_3^*), \\ F_2 &= -(a_5 - a_5^*). \end{aligned} \quad (\text{A5})$$

APPENDIX B

Using Eqs. (2.11) we obtain the result that, near the second-order phase transition, $a = A_1 + B_2q_0 + D_1q_0^2 = 0$ with q_0 being a solution of $A_2 + B_2q_0 + D_2q_0^2 + F_2q_0^3 = 0$. To obtain the expression for b , one has to solve Eq. (2.9) for small m . The solution is of the form

$$q = q_0 + q_1m^2, \quad (\text{B1})$$

where q_1 is given by

$$q_1 = -\frac{C_2 + q_0E_2}{B_2 - 2D_2q_0 + 3F_2q_0^2}. \quad (\text{B2})$$

This yields

$$3b = B_1q_1 + 2D_1q_1 + C_1. \quad (\text{B3})$$

* Electronic address: jfmendes@fc.up.pt

- [1] T. M. Liggett, *Interacting Particle Systems*, A Series of Comprehensive Studies in Mathematics Vol. 296 (Springer-Verlag, Berlin, 1985).
- [2] P. L. Garrido, J. Marro, and J. M. González-Miranda, *Phys. Rev. A* **40**, 5802 (1984); Jian-Sheng Wang and J. L. Lebowitz, *J. Stat. Phys.* **51**, 893, (1988); J. M. González-Miranda, P. L. Garrido, J. Marro, J. L. Lebowitz, *Phys. Rev. Lett.* **59**, 1934 (1987).
- [3] J. M. González-Miranda and J. Marro, *J. Stat. Phys.* **61**, 1283 (1990).
- [4] R. Schlögl, *Z. Phys.* **253**, 147 (1972).
- [5] R. Bidaux, N. Boccara, and H. Chaté, *Phys. Rev. A* **39**, 3094 (1989).
- [6] R. Dickman and Tania Tomé, *Phys. Rev. A* **44**, 4833 (1991).
- [7] M. Blume, V. J. Emery, and R. B. Griffiths, *Phys. Rev. A* **4**, 1071 (1971).
- [8] J. R. Glauber, *J. Math. Phys.* **4**, 294 (1963).
- [9] K. Kawasaki, *Phys. Rev.* **145**, 224 (1966).
- [10] J. F. F. Mendes and E. J. S. Lage (unpublished).
- [11] A. De Masi, P. A. Ferrari, and J. L. Lebowitz, *J. Stat. Phys.* **44**, 589 (1986); *Phys. Rev. Lett.* **55**, 463 (1985).
- [12] Katsumi Kasomo and Ikuo Ono, *Z. Phys. B* **88**, 205 (1992).
- [13] R. Dickman, *Phys. Lett. A* **122**, 463 (1987).
- [14] M. Droz, Z. Rácz, and P. Tartaglia, *Phys. Rev. A* **41**, 6621 (1990).
- [15] H. Sponh, *Rev. Mod. Phys.* **53**, 569 (1980).